AMERICAN SOCIETY FOR MICROBIOLOGY | Journal of Virology®

CD8$^+$ T Cell Immune Response in Immunocompetent Mice during Zika Virus Infection

Huarong Huang,[a,b] Shihua Li,[a] Yongli Zhang,[e] Xiaojuan Han,[a,b] Baoqian Jia,[a] Hongtao Liu,[a,b] Dandan Liu,[a,b] Shuguang Tan,[a] Qihui Wang,[a] Yuhai Bi,[a] William J. Liu,[e] Baidong Hou,[c] George Fu Gao,[a,d,e,f] Fuping Zhang[a,d]

CAS Key Laboratory of Pathogenic Microbiology and Immunology, Institute of Microbiology, Chinese Academy of Sciences, Beijing, China[a]; University of Chinese Academy of Sciences, Beijing, China[b]; Institute of Biophysics, Chinese Academy of Sciences, Beijing, China[c]; Savaid Medical School, University of Chinese Academy of Sciences, Beijing, China[d]; National Institute for Viral Disease Control and Prevention, Chinese Center for Disease Control and Prevention, Beijing, China[e]; Research Network of Immunity and Health, Beijing Institutes of Life Science, Chinese Academy of Sciences, Beijing, China[f]

ABSTRACT Zika virus (ZIKV) infection causees neurologic complications, including Guillain-Barré syndrome in adults and central nervous system (CNS) abnormalities in fetuses. We investigated the immune response, especially the CD8$^+$ T cell response in C57BL/6 (B6) wild-type (WT) mice, during ZIKV infection. We found that a robust CD8$^+$ T cell response was elicited, major histocompatibility complex class I-restricted CD8$^+$ T cell epitopes were identified, a tetramer that recognizes ZIKV-specific CD8$^+$ T cells was developed, and virus-specific memory CD8$^+$ T cells were generated in these mice. The CD8$^+$ T cells from these infected mice were functional, as evidenced by the fact that the adoptive transfer of ZIKV-specific CD8$^+$ T cells could prevent ZIKV infection in the CNS and was cross protective against dengue virus infection. Our findings provide comprehensive insight into immune responses against ZIKV and further demonstrate that WT mice could be a natural and easy-access model for evaluating immune responses to ZIKV infection.

IMPORTANCE ZIKV infection has severe clinical consequences, including Guillain-Barré syndrome in adults, microcephaly, and congenital malformations in fetuses and newborn infants. Therefore, study of the immune response, especially the adaptive immune response to ZIKV infection, is important for understanding diseases caused by ZIKV infection. Here, we characterized the CD8$^+$ T cell immune response to ZIKV in a comprehensive manner and identified ZIKV epitopes. Using the identified immunodominant epitopes, we developed a tetramer that recognizes ZIKV-specific CD8$^+$ T cells *in vivo*, which simplified the detection and evaluation of ZIKV-specific immune responses. In addition, the finding that tetramer-positive memory CD8$^+$ T cell responses were generated and that CD8$^+$ T cells can traffic to a ZIKV-infected brain greatly enhances our understanding of ZIKV infection and provides important insights for ZIKV vaccine design.

KEYWORDS CD8$^+$ T cell, ZIKV, central nervous system, cross protection, immunocompetent mouse model

Zika virus (ZIKV) is a mosquito-transmitted flavivirus and a member of the *Flaviviridae* family of positive-stranded RNA enveloped viruses; the virus has also been found to be sexually and vertically transmitted (1). It was identified in 1947 in sentinel monkeys in Uganda (2). After its introduction into Brazil in 2015, ZIKV spread rapidly, both (i) causing a mild syndrome characterized by self-limiting fever, headache, myalgia, rash, and conjunctivitis and (ii) resulting in severe clinical consequences, including Guillain-

Received 2 June 2017 **Accepted** 17 August 2017

Accepted manuscript posted online 23 August 2017

Citation Huang H, Li S, Zhang Y, Han X, Jia B, Liu H, Liu D, Tan S, Wang Q, Bi Y, Liu WJ, Hou B, Gao GF, Zhang F. 2017. CD8+ T cell immune response in immunocompetent mice during Zika virus infection. J Virol 91:e00900-17. https://doi.org/10.1128/JVI.00900-17.

Editor Michael S. Diamond, Washington University School of Medicine

Address correspondence to George Fu Gao, gaof@im.ac.cn, or Fuping Zhang, zhangfp@im.ac.cn.

H.H. and S.L. contributed equally to this article.

Barré syndrome (GBS), in adults and microcephaly and congenital malformations in fetuses and newborn infants (3, 4).

The currently popular *H-2*^{b} mouse models of ZIKV infection have recently been established in mice treated with blocking anti-IFNAR monoclonal antibody or in gene-deficient mice that globally lack IFNAR (5, 6). Neonatal B6 wild-type (WT) mice have been used as a ZIKV infection model. However, the immune systems of these mice are underdeveloped, which means that these mice are also immunocompromised (7). Recently, two additional groups demonstrated that CD8^{+} T cells can be activated by ZIKV infection in WT mice (8, 9). However, the function of WT CD8^{+} T cells was not addressed in these two reports, and whether memory CD8^{+} T cells are generated in WT mice during ZIKV infection has never been reported.

With the emergence of new disease syndromes caused by and associated with ZIKV and dengue virus (DENV) infections, it is important to address the role of CD8^{+} T cell responses to understand ZIKV immunology and pathogenesis. The protective role of the CD8^{+} T cell immune response against ZIKV was well demonstrated in LysMCre^{+} IFNAR$^{fl/fl}$ mice (5). However, it has been reported that the CD8^{+} T cell response was amplified during DENV infection in LysMCre^{+} IFNAR$^{fl/fl}$ mice (10). In addition, due to the similarity of ZIKV and DENV, the cross-reactivity of the CD8^{+} T cell immune response to ZIKV also needs to be studied. Wen et al. demonstrated that DENV immune CD8^{+} T cells were cross-reactive to ZIKV in *Ifnar1*$^{-/-}$ mice (11). Whether the cross-reactivity can be induced in WT mouse and whether cross-reactivity of the CD8^{+} T cell response to ZIKV can protect host against DENV infection are still unclear. Furthermore, ZIKV infection can cause severe nerve disorders by infecting the central nervous system (CNS) (6), but whether the CD8^{+} T cell response is involved in controlling the virus in a ZIKV-infected CNS remains undetermined.

We report here that ZIKV successfully infected WT mice and induced robust CD8^{+} T cell responses. We identified and validated CD8^{+} T cell epitopes of ZIKV and developed a tetramer that is specifically recognized by ZIKV-infected CD8^{+} T cells. When ZIKV infected the CNS, numerous virus-specific CD8^{+} T cells were recruited to the brain and spinal cord and produced a large number of functional cytokines. Finally, the CD8^{+} T cell response was critical in preventing ZIKV infection and in cross protection against DENV infection.

RESULTS

ZIKV infected B6 WT mice and induced a robust CD8^{+} T cell response. WT mice treated with IFNAR-blocking antibody or mice genetically deficient in IFNAR are currently popular animal models for investigating the immune response and pathogenesis of ZIKV infection (5, 6), although two papers reported recently that CD8^{+} T cells could be activated by ZIKV infection in B6 WT mice (8, 9). Numerous studies have demonstrated that type I interferon (IFN) deficiency impaired the CD8^{+} T cell response during virus infection through many cellular and molecule mechanisms, such as by impairing the priming effect of dendritic cells and upregulating the expression of the inhibitory molecules PD-1 and Tim3 of CD8^{+} T cells during virus infection (10, 12, 13). In addition, because of the deficiency of innate immune components, the IFNAR knockout (KO) mouse model could exclude a comprehensive study of the immune response (14, 15) and did not reflect the natural immune response after infection. Therefore, we sought to investigate whether a CD8^{+} T cell response can be induced in WT mice. To do this, 5-week-old B6 WT mice were infected with ZIKV intraperitoneally (i.p.), and body weight was monitored every day. We found that all of the mice infected with ZIKV showed mild inhibition of body weight growth (Fig. 1a) and splenomegaly at day 7 compared to that of mock-treated mice (Fig. 1b). We detected the viral load by both plaque assay and quantitative reverse transcription-PCR (qRT-PCR); as a result, no infectious virus was detected by 2 or 3 days postinfection (dpi) in the spleen, spinal cord, or brain (date not shown), which is similar to previous findings (6). However, viral RNA could be detected by qRT-PCR in the spleen but not in the spinal cord or brain at 3 dpi (Fig. 1c), whereas

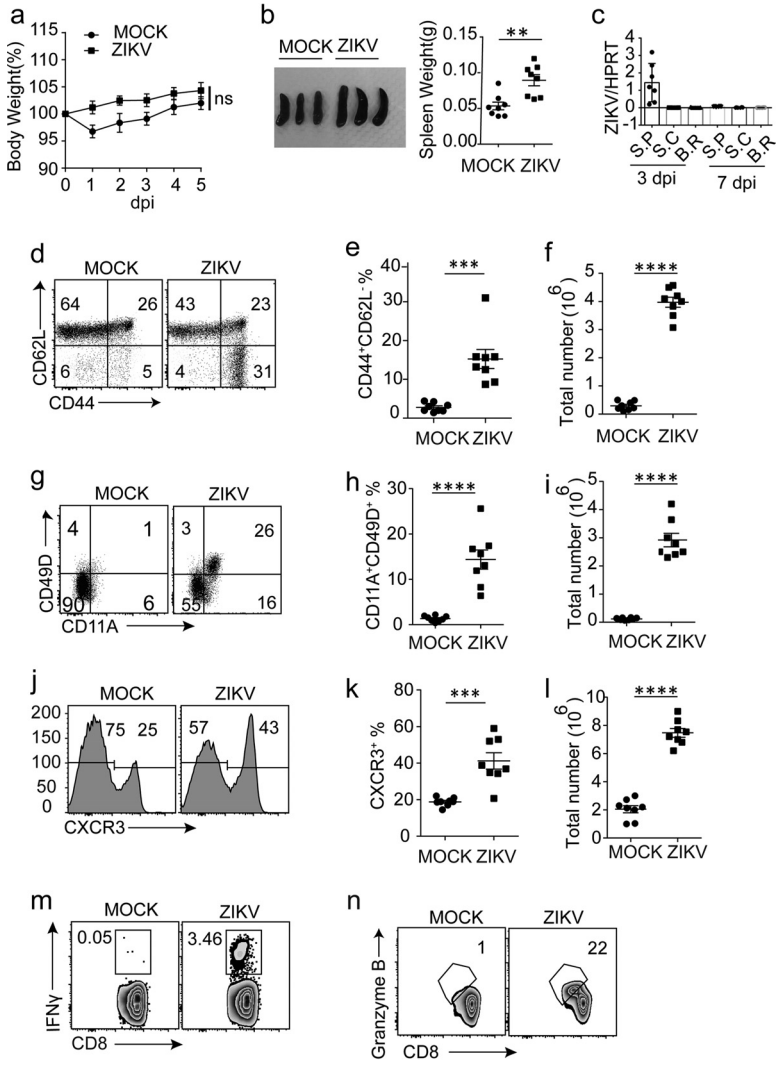

FIG 1 Robust CD8+ T cell response caused by ZIKV infection in WT B6 mice. Five-week-old B6 WT mice were infected with 2×10^6 PFU of ZIKV. "Mock" represents control mice injected with PBS. (a) Body weight. (b) Splenomegaly (left) and quantification of spleen weight (right). Mice were sacrificed at 7 dpi, and ZIKV-infected and mock-treated mice were compared. (c) ZIKV RNA levels in the spleen, spinal cord, and brain were quantified by real-time qRT-PCR. Data are presented as ZIKV units normalized to HPRT levels. S.P., spleen; S.C., spinal cord; B.R., brain. Splenocytes were obtained from ZIKV-infected and mock-treated mice at 7 dpi and analyzed for the expression of $CD44^{high}$ $CD62L^{low}$ (gated on $CD8^+$ T cells) (d), quantification of the frequency of $CD44^{high}$ $CD62L^{low}$ (e), and quantification of the numbers of $CD44^{high}$ $CD62L^{low}$ $CD8^+$ cells (f). (g) Expression of $CD11a^+$ $CD49d^+$ (gated on $CD8^+$ T cells). (h) Quantification of the frequency of $CD11a^+$ $CD49d^+$. (i) Quantification of the numbers of $CD11a^+$ $CD49d^+$ $CD8^+$ cells. (j) Expression of $CXCR3^+$ cells (gated on $CD8^+$ T cells). (k) Quantification of the frequency of $CXCR3^+$ cells. (l) Numbers of $CXCR3^+CD8^+$ cells. (m) Expression of ZIKV-specific IFN-γ^+ $CD8^+$ T cells after splenocytes from ZIKV-infected mice were stimulated with heat-inactivated ZIKV-treated DC2.4 cells. (n) Expression of granzyme B^+ $CD8^+$ T cells of ZIKV-infected and mock-treated mice. Error bars represent means ± the SEM. Data have been pooled from three independent experiment. $n = 2$ to 3 mice per group per experiment. Data were analyzed by Student t test (**, $P < 0.01$; ***, $P < 0.001$; ****, $P < 0.0001$).

at 7 dpi, the ZIKV was completely undetectable. These results indicated that ZIKV could infect and transient replicate in B6 WT mice.

We next investigated whether ZIKV infection could induce immune responses. Virus infection can result in activation and proliferation of virus-specific $CD8^+$ T cells. Once T cells are activated, the expression of CD44 increases and that of CD62L decreases (16, 17). We found that both the percentage and the total number of $CD8^+$ $CD44^{hi}$ $CD62L^{low}$ cells dramatically increased by 7 dpi (Fig. 1d to f). In addition, CD11a and CD49d, antigen-experienced markers (17), were also significantly upregulated in ZIKV-

infected WT mice (Fig. 1g to i). Finally, CXCR3, a functional molecule that can promote $CD8^+$ T cell migration to infection sites (18), was greatly induced after ZIKV infection (Fig. 1j to l). In additional studies, splenocytes from ZIKV-infected mice were stimulated with DC2.4 cells that was pretreated with heat-inactivated ZIKV and analyzed by flow cytometry. We found that a large amount of virus-specific IFN-γ-producing $CD8^+$ T cells were generated (Fig. 1m). In addition, the percentages of granzyme B^+ $CD8^+$ T cells was also dramatically increased (Fig. 1n). These results further demonstrate that although ZIKV infection in immunocompetent mice caused very mild symptoms, it did induce a robust $CD8^+$ T cell immune response.

Kinetics of the $CD8^+$ T cell response in WT B6 mice during ZIKV infection. To further investigate the $CD8^+$ T cell response to ZIKV infection, B6 WT mice were infected with ZIKV either i.p. or subcutaneously (s.c.) (19), and the $CD8^+$ T cell response was detected at 0, 4, 7, and 10 dpi. We found that the percentage of $CD8^+$ $CD44^{hi}$ $CD62L^{low}$ T cells peaked at day 7 and decreased by day 10 (Fig. 2a and b). Similar expression patterns of CD11a, CD49d, and CXCR3 in $CD8^+$ T cells in ZIKV-infected mice were observed (Fig. 2c to f). Furthermore, functional cytokine gamma interferon (IFN-γ) produced by $CD8^+$ T cell after virus infection were also analyzed at day 7 (Fig. 2g and 2h). These results indicated that a strong and rapid $CD8^+$ T cell response to ZIKV infection was developed in immunocompetent mice by when using both i.p. and s.c. infection routes.

Identification and characteristic of ZIKV-derived epitopes recognized by $CD8^+$ T cells in B6 WT mice. The structural envelope glycoprotein (E protein) of ZIKV functions in receptor binding, membrane fusion, and viral assembly (20), which suggests that this protein might be immunodominant. In addition, nonstructural protein NS2A is involved in viral RNA replication, virus assembly, and secretion. Therefore, E protein and NS2A were chosen. Ten peptides in total were designed from these proteins using the IEDB website (http://www.iedb.org/). Splenocytes obtained from ZIKV-infected B6 WT mice were stimulated with each peptide, respectively, and the levels of IFN-γ^+ among $CD8^+$ T cells were assessed. Six of the 10 ZIKV-derived peptides induced IFN-γ-producing $CD8^+$ T cells (Fig. 3a and b). Of these six peptides (Table 1), the epitope E_{4-12} induced the highest IFN-γ-producing cells (i.e., 3 to 4% IFN-γ^+ $CD8^+$ cells after ZIKV infection), suggesting the immunodominance of E_{4-12} epitope among positive peptides we identified. This finding was also consistent with Pardy's report that the E_{4-12} epitope was recognized by a majority of responding cells during ZIKV infection (9). Two peptides derived from the E protein (E_{4-12} and $E_{310-317}$) and one from NS2A ($NS2A_{91-98}$) of our virus strain are consistent with a recent report (5). Two NS2A epitopes ($NS2A_{34-41}$ and $NS2A_{43-51}$) and one E protein epitopes ($E_{204-212}$) have never been reported. Tetramer was used to detect and quantify T cells that are specific for a given antigen, which simplifies the detection and evaluation of antigen-specific immune responses. Using the immunodominant epitope E_{4-12}, ZIKV tetramer was synthesized. We found that E_{4-12} tetramer-positive $CD8^+$ T cells were detected in the splenocytes of ZIKV-infected mice but not in control mice (Fig. 3c and d), which suggests that the E_{4-12} tetramer could be recognized by ZIKV-specific $CD8^+$ T cells and used to evaluate the immune response after ZIKV infection.

The functions of $CD8^+$ T cells against virus-infected cells are associated with the production of cytokines such as IFN-γ, tumor necrosis factor alpha (TNF-α), and interleukin-2 (IL-2) (21). Degranulation of effector $CD8^+$ T cells is also important for killing virus-infected cells. Therefore, we extended our study by examining the expression of CD107a and IFN-γ in ZIKV-specific $CD8^+$ T cells in B6 WT mice at days 4, 7, and 10 by restimulating the splenocytes with screened peptides. Consistent with the above findings, CD107a- and IFN-γ-producing $CD8^+$ T cells were induced and peaked at day 7, followed by downregulation at day 10 (Fig. 3e and f).

The cytotoxic-T-lymphocyte (CTL) effect was an important function of effector $CD8^+$ T cells during infection and used to evaluate ZIKV vaccine candidates. However, the CTL effect of WT $CD8^+$ T cells during ZIKV infection remains undefined, although this effect

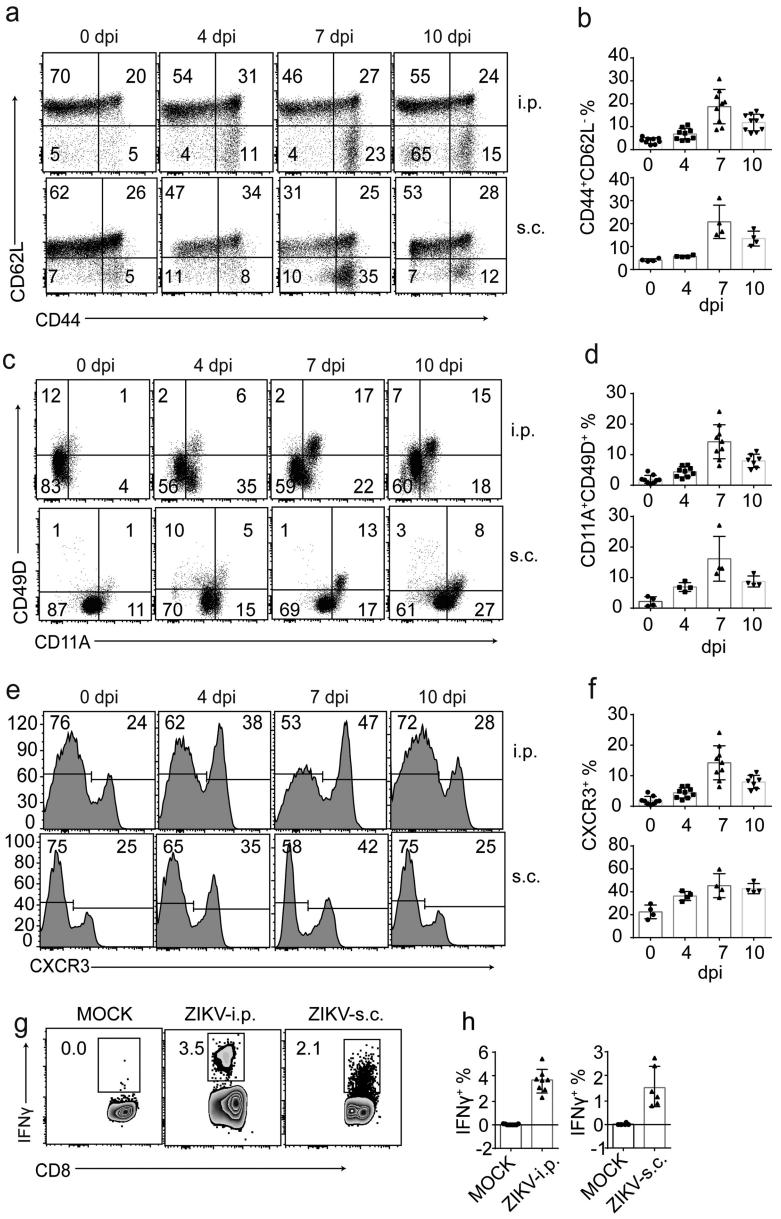

FIG 2 Kinetics of the CD8+ T cell response to ZIKV infection in WT B6 mice. B6 WT mice were infected with 2×10^6 PFU of ZIKV either i.p. or s.c. Splenocytes were obtained at 0, 4, 7, and 10 dpi. (a, c, and e) Expression of $CD44^{high}$ $CD62L^{low}$ (a), $CD11a^+$ $CD49d^+$ (c), and $CXCR3^+$ (e) at the indicated time points (gated on $CD8^+$ T cells). (b, d, and f) Quantification of the frequencies of $CD44^{high}$ $CD62L^{low}$ $CD8^+$ (b), $CD11a^+$ $CD49d^+$ $CD8^+$ (d) and $CXCR3^+$ $CD8^+$ (f) T cells. (g) Expression of ZIKV-specific IFN-γ^+ of $CD8^+$ T cells. Splenocytes from ZIKV-infected mice were stimulated with heat-inactivated ZIKV-treated DC2.4 cells. (h) Quantification of IFN-γ^+ $CD8^+$ T cells. Error bars represent means ± the SEM. Data are pooled from two or three independent experiments. $n = 2$ to 3 mice per group per experiment.

was well documented in $LysMCre^+$ $IFNAR^{fl/fl}$ mice (5). Therefore, we sought to analyze the cytolytic activity of the ZIKV-specific WT $CD8^+$ T cells. Briefly, CFSE (carboxyfluorescein succinimidyl ester)-labeled splenocytes pulsed with individual positive peptides were adoptively transferred into ZIKV-infected WT B6 mice, and the percentage of the target cell killing was calculated after 13 h of cell transfer (Fig. 3g and 3h). Among the peptides used in the assay, E_{4-12} produced the strongest CTL effect.

Taken together, six ZIKV epitopes restricted to $CD8^+$ T cells were identified in immunocompetent mice. Of the six peptides, E_{4-12} produced the strongest CTL effect, indicating that this epitope is immunodominant. Furthermore, a ZIKV-specific tetramer was developed that will facilitate ZIKV research in the future.

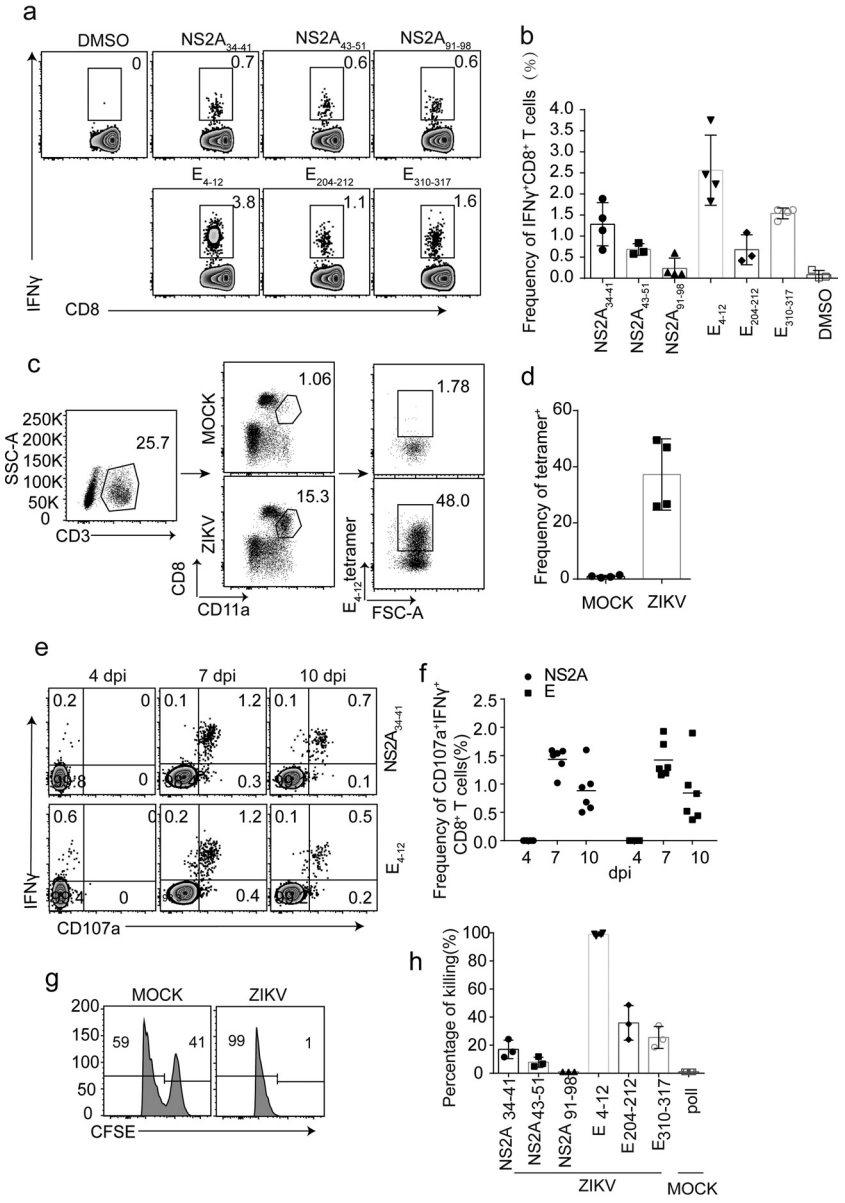

FIG 3 Identification and characteristics of ZIKV-derived epitopes recognized by CD8$^+$ T cells in B6 WT mice. FIve-week-old B6 WT mice were infected with 2×10^6 PFU of ZIKV and analyzed at 7 dpi. (a) Representative plots of IFN-γ of CD8$^+$ T cells. Splenocytes from infected mice were stimulated with peptides derived from ZIKV strain SMGC-1. (b) Quantification of the frequency of IFN-γ^+ cells among CD8$^+$ T cells. (c) Representative plots of E_{4-12} tetramer-positive cells. The staining gating strategy is indicated. (d) Quantification of the frequency of E_{4-12} tetramer-positive cells among CD3$^+$ CD8^{low} CD11a$^+$ T cells. (e) Expression of CD107a$^+$ IFN-γ^+ among CD8$^+$ T cells. (f) Quantification of the frequency of CD107a$^+$ IFN-γ^+ among CD8$^+$ T cells at the designated time points after ZIKV infection. (g and h) *In vivo* killing of ZIKV peptide-pulsed cells. WT B6 mice infected 7 days previously with 2×10^6 PFU of ZIKV were injected i.v. with CFSE-labeled target cells pulsed with the designated peptides. After 13 h, the splenocytes were harvested and analyzed by flow cytometry, and the percent killing was calculated. (g) Representation of *in vivo* killing of target cells in ZIKV-infected mice. (h) Quantification of the percentage of killing. Error bars represent means ± the SEM. Data are pooled from two independent experiments. $n = 2$ to 3 mice per group per experiment.

ZIKV and DENV epitope-specific CD8$^+$ T cell responses were mutually cross-reactive in a WT mouse. Several studies have demonstrated a close antigenic relationship between ZIKV and DENV, with potential implications for vaccines and therapeutics (22, 23). Most of these studies focused on the cross talk of neutralizing antibodies between ZIKV and DENV and the structural basis for such cross-reactivity. A very recent study of ZIKV reported that DENV-specific CD8$^+$ T cell epitopes were

TABLE 1 ZIKV-derived peptides[a]

Peptide	Sequence	Length (nt)
ZK-NS2A-34	ISTSMAVL	8
ZK-NS2A-43	AMILGGFSM	9
ZK-NS2A-91	VSFIFRAN	8
ZK-E-4	IGVSNRDFV	9
ZK-E-204	LTMNNKHWL	9
ZK-E-310	AAFTFTKI	8

[a]Peptides from ZIKV strain SMGC-1 were predicted to bind to *H-2*^{b} class I molecules (Db and Kb). nt, nucleotides.

cross-reactive to ZIKV, and this was also demonstrated in *Ifnar1*$^{-/-}$ mice (11). In the present study, we sought to investigate whether such cross-reactivity of CD8$^+$ T cells can be observed in WT mice. First, splenocytes isolated from DENV-infected WT mice were stimulated with peptides derived from ZIKV. We found that IFN-γ^+ CD8$^+$ T cells were produced, suggesting that CD8$^+$ T cell responses generated in DENV infection were cross-reactive to ZIKV in WT mice (Fig. 4a). Given the coincidence of ZIKV and DENV infection, we examined whether cross-reactivity of CD8$^+$ T cell responses

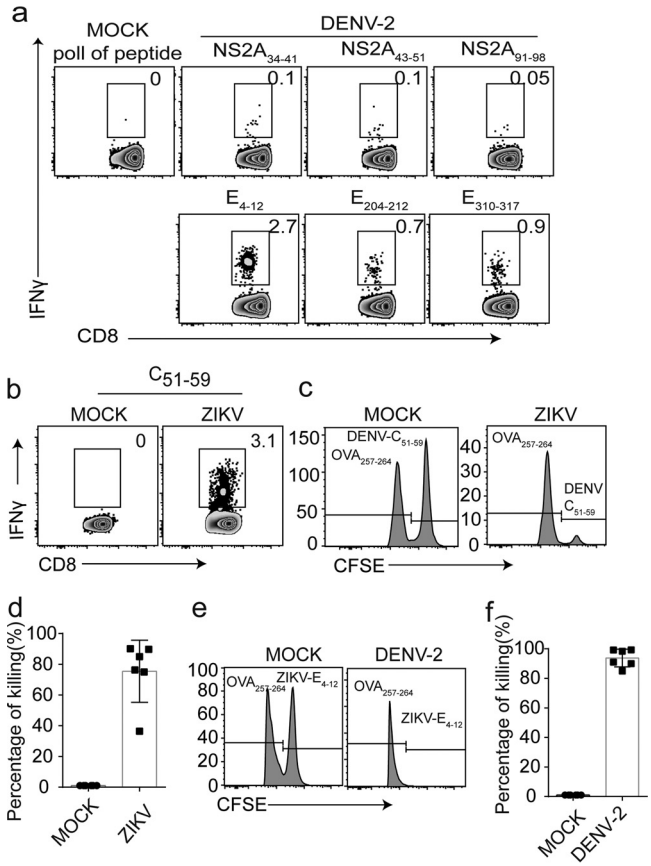

FIG 4 The ZIKV and DENV epitope-specific CD8$^+$ T cell response was mutually cross-reactive in the WT mouse model. (a) Expression of IFN-γ^+ among CD8$^+$ T cells. Five-week-old B6 WT mice were infected with 2×10^6 PFU of DENV-2, the mice were sacrificed, and splenocytes were harvested at 7 dpi and stimulated with ZIKV-derived CD8$^+$ peptides. "Mock" represents control mice injected with PBS. IFN-γ^+ CD8$^+$ T cells were detected by intracellular staining. (b) Expression of IFN-γ^+ among CD8$^+$ T cells. Five-week-old B6 WT mice were infected with 2×10^6 PFU of ZIKV. "Mock" represents control mice injected with PBS. Mice were sacrificed, and splenocytes were harvested at 7 dpi and stimulated with DENV-2-derived CD8$^+$ peptide, as indicated in the figure. (c and e) *In vivo* killing of target cells pulsed with peptide C_{51} derived from DENV-2 and peptide E_{4-12} derived from ZIKV in ZIKV-infected mice (c) and DENV-2 infected mice (e), respectively. (d) Quantification of panel c. (f) Quantification of panel e. Error bars represent means ± the SEM. Data are pooled from two independent experiments. $n = 3$ mice per group per experiment.

were mutual between ZIKV and DENV infection. Splenocytes from ZIKV-infected WT mice were stimulated with the previously reported DENV peptide C_{51-59} (24), and a very similar cross-reaction was observed (Fig. 4b).

Next, we detected the cross-CTL effect of $CD8^+$ T cells by carrying out an *in vivo* killing assay. CFSE-labeled splenocytes pulsed with peptide C_{51-59} derived from DENV-2 (DENV strain 43, GenBank accession number AF204178) were first transferred into ZIKV-infected WT B6 mice. Then, the percentage of target cell killing was calculated after 13 h of cell transfer. The results indicated that the $CD8^+$ T cell response to ZIKV could have a CTL effect on DENV-primed cells (Fig. 4c and d). In addition, the CTL effect derived from DENV-2 infection could also kill ZIKV peptide-pulsed splenocytes (Fig. 4e and f).

The epitope E_{4-12} derived from ZIKV mediated the strongest cross-reactivity. The amino acids sequence comparison showed that E_{4-12} is highly conserved between ZIKV and DENV-2, sharing 88.9% identity. Other peptides were also cross-reactive but to a lower extent (Fig. 4a and b), which indicated that the epitopes E_{4-12} of ZIKV screened in WT mouse model could be a very good candidate for vaccine.

Memory $CD8^+$ T cells developed after ZIKV infection. It is well known that long-term immune protection depends on the quantity and quality of memory T cells developed after infection or vaccination. Memory T cells can rapidly acquire effector functions to kill infected cells and/or secrete inflammatory cytokines (25, 26). ZIKV infection induces a rapid and strong $CD8^+$ T cell immune response in WT mice. However, whether ZIKV infection can induce memory $CD8^+$ T cell development has never been reported. Therefore, we evaluated memory $CD8^+$ T cells in ZIKV-infected WT mice. Splenocytes isolated from ZIKV infected mice at days 35 and 60 were stimulated with ZIKV-specific peptide, and IFN-γ^+ virus-specific memory $CD8^+$ T cells were detected (Fig. 5a and b). Importantly, we observed ZIKV-specific memory $CD8^+$ T cells even at 140 dpi by both E_{4-12} tetramer and IFN-γ staining (Fig. 5c to f), Taken together, these results indicated that a long-term memory $CD8^+$ T cell response could develop during ZIKV infection in immunocompetent mice.

$CD8^+$ T cell immune response in ZIKV-infected CNS. Recently, more studies have reported that a $CD8^+$ T cell response is induced in the CNS after virus infection in spite of its immune-privileged specificity. Such immune responses in the CNS need to be under strict control because the immunopathological damage of this organ during an active immune response must be kept to a minimum (27, 28). During a ZIKV outbreak, an increased incidence of Guillain-Barré syndrome (GBS) was reported (29), and $CD8^+$ T cells play a very important role in GBS (30). Therefore, to further study the function of the ZIKV-specific $CD8^+$ T cell immune response in the CNS, we used *Ifnar1*$^{-/-}$ mice because previous studies have demonstrated that ZIKV infection in this mouse could cause severe pathogenesis in the CNS (6). We studied the $CD8^+$ T cell immune responses in the CNSs of ZIKV-infected *Ifnar1*$^{-/-}$ and WT B6 mice. We found that the immune response in the CNSs of ZIKV infected *Ifnar1*$^{-/-}$ mice was quite different from that of B6 WT mice. A large number of lymphocytes and $CD8^+$ T cells infiltrated the spinal cords and brains of ZIKV-infected *Ifnar1*$^{-/-}$ mice but were absent in WT mice (Fig. 6a and b). The $CD8^+$ IFN-γ^+ T cells in the CNS were CD11a positive and polyfunctional since they were IFN-γ^+ $CD107a^+$ cells after stimulation with virus-specific peptide (Fig. 6c and d). These results seem to be due to the high levels of ZIKV in the CNSs of *Ifnar1*$^{-/-}$ mice and the undetectable virus in the CNSs of WT mice (Fig. 1c). Finally, CNS-infiltrated $CD8^+$ T cells are ZIKV-specific $CD8^+$ T cells since they are E_{4-12} tetramer-positive cells (Fig. 6e). To further study the infiltration and cytokine secretion patterns of $CD8^+$ T cells in the spinal cord and brain, *Ifnar1*$^{-/-}$ mice were infected with ZIKV, and the $CD8^+$ T cell responses in the CNS were measured at different time points. We found that lymphocytes (Fig. 6f) and $CD8^+$ T cells started to infiltrate the CNS and secrete polyfunctional cytokines at 4 dpi, peaked at around 7 dpi, and decreased quickly by 10 dpi (Fig. 6g to i). These data suggested that $CD8^+$ T cells could be recruited to the CNS during ZIKV infection.

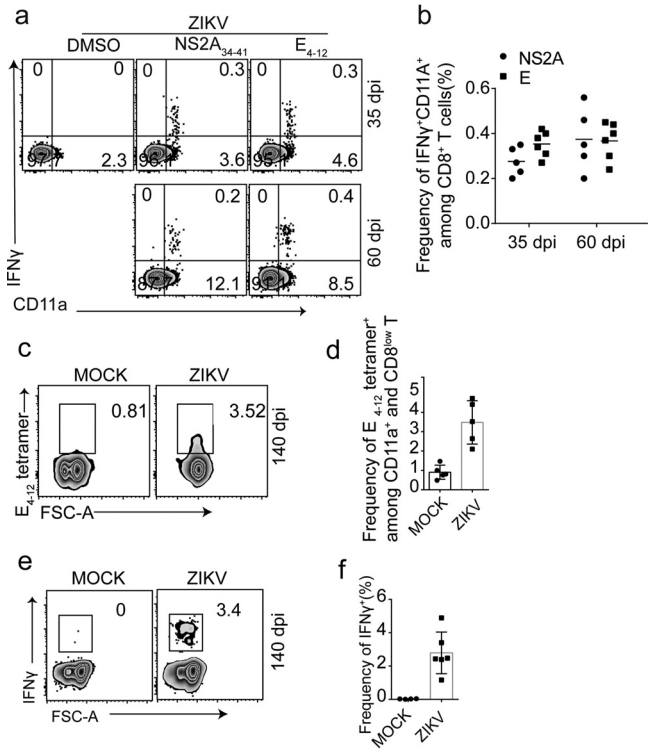

FIG 5 Memory CD8$^+$ T cells were developed during ZIKV infection. (a) Representative zebra plot showing the expression of CD11a$^+$ IFN-γ^+ among CD8$^+$ T cells after stimulation with peptide derived from ZIKV. (b) Quantification of the frequency of CD11a$^+$ IFN-γ^+ among CD8$^+$ T cells. B6 WT mice were infected with 2×10^6 PFU of ZIKV. Splenocytes were obtained at 35 and 60 dpi and stimulated with peptides derived from ZIKV. Memory CD8$^+$ T cells were evaluated by IFN-γ^+ CD11a$^+$ double-positive cells. (c) Representative plots of E_{4-12} tetramer-specific CD8$^+$ memory cells at 140 dpi (gated on CD3$^+$ CD8^{low} CD11a$^+$ cells). (d) Quantification of the frequency of E_{4-12} tetramer$^+$ among CD3$^+$ CD8^{low} CD11a$^+$ cells. (e) Representative zebra plot showing the expression of IFN-γ^+ gated on CD3$^+$ CD8^{low} CD11a$^+$ cells after stimulation with peptide E_{4-12}. (f) Quantification of the frequency of IFN-γ^+ cells among CD3$^+$ CD8^{low} cd11a$^+$ cells. Error bars represent means $\pm$ the SEM. Data are pooled from two independent experiments. $n = 3$ mice per group per experiment.

Role of the CD8$^+$ T cell response during ZIKV infection. Having found that CD8$^+$ T cells infiltrated the CNSs of ZIKV-infected *Ifnar1*$^{-/-}$ mice, we then investigated the importance of CD8$^+$ T cells in controlling virus infection in the CNS. Briefly, 10^7 CD8$^+$ T cells isolated from ZIKV-infected or noninfected B6 WT mice, respectively, were transferred into *Ifnar1*$^{-/-}$ mice, and then the recipient *Ifnar1*$^{-/-}$ mice were infected with ZIKV 1 day after cell transfer. Body weight, virus load, and the immune response of CD8$^+$ T cells in the CNS were investigated. We found that *Ifnar1*$^{-/-}$ mice adoptively transferred with ZIKV-infected CD8$^+$ T cells were protected from body weight loss (Fig. 7a) and a decreased ZIKV burden in the spinal cords and brains of mice adoptively transferred with CD8$^+$ T cells compared to noninfected mice (Fig. 7b and c). In addition, the levels of both lymphocytes and CD8$^+$ T cells also decreased significantly in the spinal cords and brains of mice adoptively transferred with ZIKV-infected CD8$^+$ T cells compared to those of mice adoptively transferred with noninfected CD8$^+$ T cells (Fig. 7d and e). These results demonstrated that CD8$^+$ T cells are critical to prevent ZIKV infection.

A recent publication showed that ZIKV/DENV cross-reactive peptides immunization provided protection against ZIKV infection (11). However, whether the cross talk mediated by CD8$^+$ T cells post-ZIKV infection could prevent DENV infection remains unclear. To investigate whether the ZIKV-specific CD8$^+$ T cells provide cross protection against DENV infection *in vivo*, 10^7 CD8$^+$ T cells derived from ZIKV-infected and noninfected B6 WT mice were adoptively transferred to *Ifnar1*$^{-/-}$ mice 1 day prior to

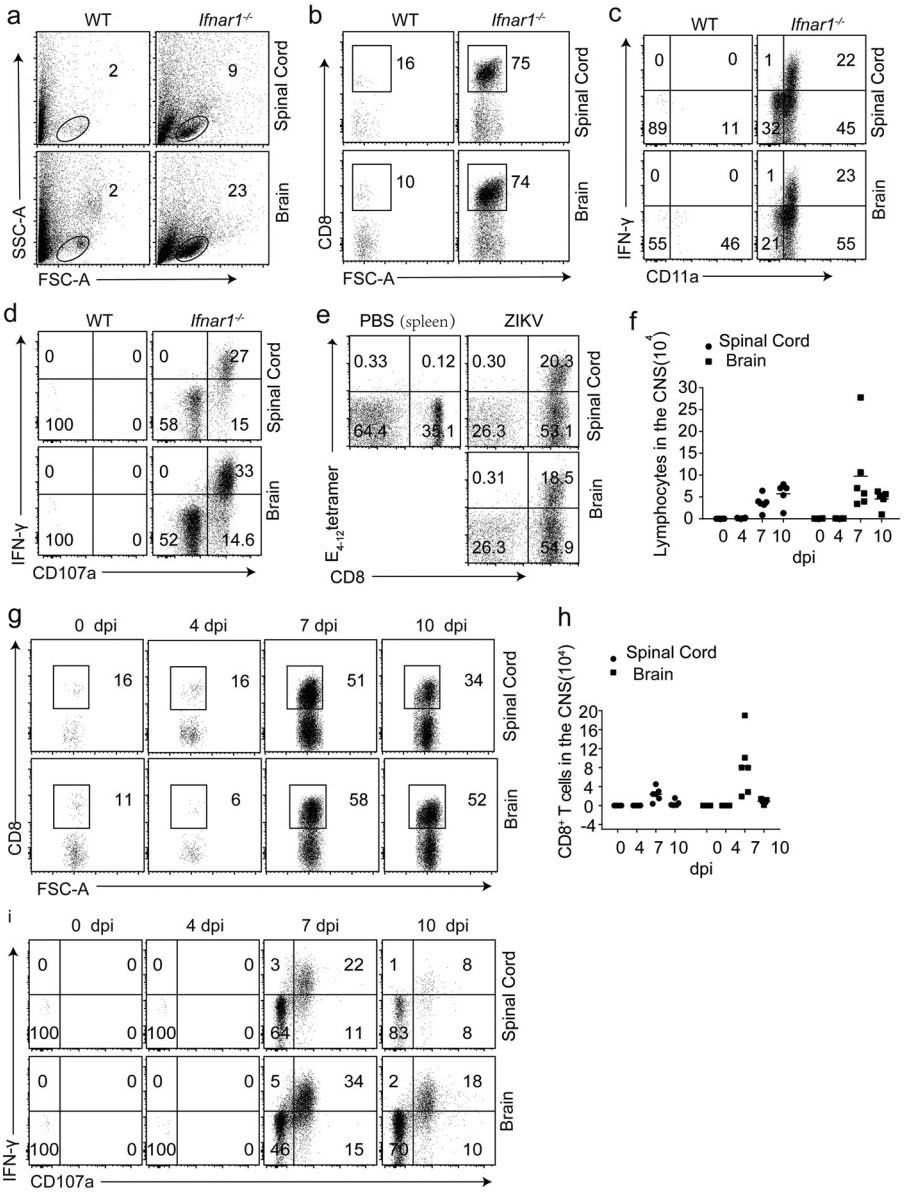

FIG 6 CD8$^+$ T cell immune response in the ZIKV-infected CNS. (a to e) B6 WT mice and *Ifnar1*$^{-/-}$ mice were infected with 10^5 PFU of ZIKV and analyzed at 7 dpi. (a and b) Representative plots of lymphocytes (a) and CD8$^+$ T cells (b) isolated from the CNS. (c and d) Expression of IFN-γ^+ CD11A$^+$ (c) and IFN-γ^+ CD107A$^+$ (d) among CD8$^+$ T cells. Lymphocytes were isolated from the spinal cord and brain and stimulated with ZIKV-derived peptide (E_{4-12}) to assess cytokine production by intracellular staining. (e) Representative plots of E_{4-12} tetramer-specific CD8$^+$ T cells in the spinal cord and brain (gated on CD3$^+$ T cells). Splenocytes obtained from noninfected mice were used as a staining negative control. (f to i) *Ifnar1*$^{-/-}$ mice were infected with 10^5 PFU of ZIKV, and analyzed lymphocytes were isolated from the spinal cord and brain at 0, 4, 7, and 10 dpi. (f) Quantification of the total number of lymphocytes. (g) Dot plot showing CD8$^+$ T cells. (h) Quantification of the number of CD8$^+$ T cells in the spinal cord or brain at the designated time points. (i) Expression of IFN-γ^+ CD107A$^+$ of CD8$^+$ T cells isolated from the spinal cord and brain and stimulated with ZIKV-derived peptide (E_{4-12}). Error bars represent means ± the SEM. Data are pooled from two independent experiments. $n = 3$ mice per group per experiment.

infection with DENV. The body weights, viral loads, and infiltrations of the CD8$^+$ T cells in the CNSs were then determined. We found that CD8$^+$ T cells obtained from ZIKV-infected mice prevented DENV-infected *Ifnar1*$^{-/-}$ mice from body weight loss (Fig. 7f) and decreased DENV burden in the brain compared to those of mice adoptively transferred with CD8$^+$ T cells from noninfected mice (Fig. 7g). Similarly, we found that both the lymphocyte and the CD8$^+$ T cell levels were decreased in the spinal cords and

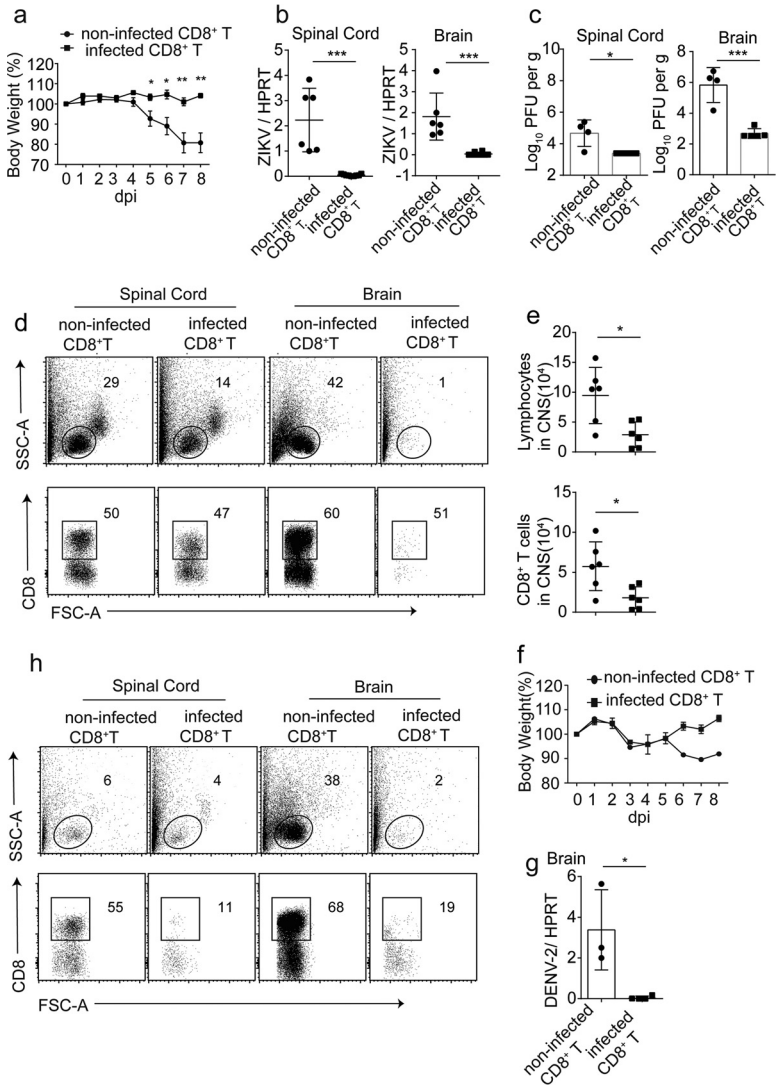

FIG 7 Role of the CD8+ T cell response during ZIKV infection. *Ifnar1*$^{-/-}$ mice were injected with ZIKV-infected CD8+ T cells and noninfected CD8+ T cells 1 day prior to infection with ZIKV, and body weights were monitored. The mice were sacrificed at day 8 for further study. (a) Body weights of mice injected with ZIKV-infected CD8+ T cells and noninfected CD8+ T cell control mice. (b and c) ZIKV load in mice injected with ZIKV-infected CD8+ T cells and noninfected CD8+ T cell control mice measured by RT-PCR and plaque-forming assay. (d) Dot plots show lymphocytes and CD8+ T cells in the CNSs of mice injected with ZIKV-infected CD8+ T cells and noninfected CD8+ T cell control mice. (e) Quantification of the total numbers of lymphocytes and CD8+ T cells in the CNSs of mice injected with ZIKV-infected CD8+ T cells and noninfected CD8+ T cell control mice. (f to h) *Ifnar1*$^{-/-}$ mice were injected with ZIKV-infected CD8+ T cells and noninfected CD8+ T cells 1 day prior to infection with 10^5 PFU of DENV-2. Their body weights were monitored, and the mice were sacrificed at 8 dpi for further study. (f) Body weight. (g) DENV-2 load in brain. (h) Representative dot plot showing the lymphocytes and CD8+ T cells isolated from the spinal cords and brains of DENV-infected mice. Error bars represent means ± the SEM. Data are pooled from two independent experiments. $n = 3$ mice per group per experiment. The data were analyzed by Student *t* test (*, $P < 0.05$; **, $P < 0.01$; ***, $P < 0.001$).

brains of mice adoptively transferred with CD8+ T cells from ZIKV-infected mice (Fig. 7h). These findings demonstrate that ZIKV cross-reactive CD8+ T cells provide cross protection against DENV infection.

DISCUSSION

Several new mouse models of ZIKV were developed over the past last year using current viral isolates. Using a Cambodian isolate of ZIKV, Rossi et al. showed that 3-week-old A129 and AG129 mice, which lack type I or I and II IFNs, respectively,

developed paralysis and succumb to disease by 7 dpi, whereas older mice showed viremia and weight loss but recovered after day 8 (31, 32). Lazear et al. assessed 4- to 6-week-old A129 or *Irf3/5/7* triple-KO mice challenged with ZIKV (H/PF/2013) from French Polynesia, as well as the African ZIKV strain MR766 (6), and similar observations were obtained. In addition, using immunocompromised neonatal mice, Mohanraj et al. showed that the mice developed clinical symptoms similar to those of of *Ifnar1*$^{-/-}$ mice after ZIKV infection (7). Therefore, the majority of mouse models used for ZIKV infection thus far are mice that lack a competent immune system (5, 6). These models are sufficient for characterizing infection and the pathogenesis of the virus because a clear infection phenotype is observed, but they are unable to provide a comprehensive and accurate understanding of the natural immune response to ZIKV infection. Recently, two reports indicated that ZIKV can infect WT mice and activate CD8$^+$ T cells (8, 9). Our studies extended these findings by characterizing the immune response to ZIKV more comprehensively in the key peripheral organs of WT adult mice. Consistent with these two reports, we also demonstrated that ZIKV infected adult B6 WT mice successfully and induced a strong CD8$^+$ T cell response; ZIKV-specific functional molecule secretion patterns by CD8$^+$ T cells peaked at day 7 and declined gradually thereafter. We screened ZIKV-specific major histocompatibility complex (MHC) class I peptides in WT mouse and identified six antigen epitopes derived from the E and NS2A proteins of ZIKV. Of these peptides, E_{4-12} induced the strongest CD8$^+$ CTL response and a ZIKV-derived E_{4-12} tetramer was first developed, which will facilitate ZIKV research in the future. Moreover, we demonstrated first that ZIKV-specific long-term memory CD8$^+$ T cells were developed during ZIKV infection. Collectively, these findings further demonstrated that WT mice could be a better model for studying the CD8$^+$ T cell immune response to ZIKV infection.

The CNS is considered to be an immune-privileged site for two reasons. First, the expression of MHC molecules is limited within the CNS parenchyma. Second, the entry of adaptive immune cells into the CNS via the blood-cerebrospinal fluid (CSF) barrier, the CSF-brain barrier, and the blood-brain barrier is restricted, but immune surveillance of the CNS does take place (33, 34). The clinical presentation of ZIKV-infected *Ifnar1*$^{-/-}$ mice, along with the previously described tropism of ZIKV for neurons, suggest that CD8$^+$ T cells may migrate to CNS when virus infects the neuron cells. Indeed, we found that a large number of CD8$^+$ T cells infiltrated in the CNS when ZIKV infected the brain or spinal cord. The CD8$^+$ T cell is important for limiting virus replication, since adoptive transfer of the virus-specific effector CD8$^+$ T cells into *Ifnar1*$^{-/-}$ mice infected with ZIKV can effectively prevent virus from infecting the CNS and reduce clinical manifestations such as weight loss and viral load. On other hand, although it is possible that the influx of T cells into the CNS plays a key role in controlling the virus and aids in the survival of the host, the presence of CD8$^+$ T cells may be driving the occurrence of GBS, given that high rates of GBS were reported during ZIKV outbreaks (29), it is highly likely that the increased incidence of GBS during ZIKV infection is associated with the pathogenic effect of virus-specific CD8$^+$ T cells in killing virus-infected neurons. Finally, the finding that the CD8$^+$ T cell response can efficiently control the ZIKV load and protect the CNS from ZIKV infection also raises an important point to be considered in evaluating and designing vaccines in the future.

ZIKV and DENV share high amino acid identity, and several recent studies demonstrated a cross-reactivity between ZIKV and DENV at the antibody response level (23). Regarding cross-reactivity in the T cell response, it has been shown that E-protein-reactive T cells directly isolated from *ex vivo* cultures of memory CD4$^+$ T cells of ZIKV- or DENV-infected human donors did not cross-react upon secondary stimulation with heterologous E proteins. These findings indicate an overall low level of CD4 T cell cross-reactivity between ZIKV and DENV E proteins (23). Considering that cocirculation of ZIKV and DENV occurs in many regions of the world due to their common vectors and geographical distributions, it is important to investigate CD8$^+$ T cell cross-reactivity and its role in the context of ZIKV infection. We showed here that the CD8$^+$ T cell immune response induced by ZIKV infection did cross-react with DENV upon secondary

stimulation with peptide from C protein of DENV. Importantly, this cross-reactivity led to cross protection against DENV infection *in vivo*, as shown by the adoptive transfer of ZIKV-infected CD8$^+$ T cells preventing weight loss in DENV-infected mice. Further study indicated that the cross protection mutually occurred between ZIKV and DENV infections. These findings suggest that the consequence of cross-reactivity elicited by a CD8$^+$ T cell response is different from that of the cross-reactive antibody: the antibody enhanced DENV infection (23), but the cross-reactivity of the CD8$^+$ T cell response to ZIKV prevented DENV infection.

The ability to develop and sustain populations of memory T cells after infection or immunization is a hallmark of the adaptive immune response and a basis for protective vaccination against infectious disease. Our data revealed that epitope-specific memory CD8$^+$ T cells were developed during ZIKV infection. These findings could provide significant insights into the development or evaluation of a novel preventive strategy against ZIKV and DENV infection. However, whether the memory CD8$^+$ T cells can prevent secondary infection needs to be further studied.

Our studies comprehensively characterized the CD8$^+$ T cell immune response during ZIKV infection in an immunocompetent mouse. The presence of infiltrating CD8$^+$ T cells in a ZIKV-infected CNS suggests that, on one hand, CD8$^+$ T cells are important for controlling virus infection but that, on the other hand, they may trigger a neurodestructive inflammatory response in the CNS. Moreover, the identification of ZIKV-specific CD8$^+$ T cell-dominant epitopes and the finding that the CD8$^+$ T cell immune response elicited by either ZIKV or DENV infection is mutually cross-reactive and cross protective provide important insight for vaccine design in the future.

MATERIALS AND METHODS

Ethics statement. All animal handling procedures were performed in compliance with People's Republic of China legislation for the care and use of laboratory animals. The experiments and protocol were approved by the Committee on the Ethics of Animal Experiments of the Institute of Microbiology, Chinese Academy of Sciences (IMCAS) under permit APIMCAS2017015. Studies with ZIKV were conducted under biosafety level 2 and animal BSL3 containment.

Cells and viruses. African green monkey kidney epithelial cells (Vero, ATCC-CCL-81) and baby hamster kidney cells (BHK-21, ATCC-CCL-10) were purchased from the American Type Culture Collection (ATCC; Manassas, VA). DC2.4 was provided by Mingzhao Zhou (Institute of Biophysics, Chinese Academy of Sciences, Beijing, China). Vero and BHK-21 cells were maintained in Dulbecco modified Eagle medium (DMEM; Invitrogen, USA) supplemented with 10% fetal bovine serum (FBS; Gibco, USA) at 37°C with 5% CO_2. ZIKV strain ZIKA-SMGC-1 (GenBank accession number KX266255) was isolated by our lab as described previously (35). DENV-2 (strain 43; GenBank accession number AF204178) was kindly provided by Cheng-Feng Qin (Beijing Institute of Microbiology and Epidemiology, Beijing, China). Virus stocks were propagated in Vero cells and titrated in BHK-21 cells by standard plaque-forming assays.

Mouse experiments. Specific-pathogen-free WT mice were supplied by the Beijing Vital River Laboratory Animal Technology Co., Ltd. (licensed by Charles River). *Ifnar1*$^{-/-}$ mice were kindly provided by Baidong Hou (Institute of Biophysics). All experiments were performed according to the institutional Animal Care and Use Committee-approved animal protocols. Five- to six-week-old female WT B6 mice and five-week-old *Ifnar1*$^{-/-}$ mice were used in this study. For infection experiments, WT B6 (female) and *Ifnar1*$^{-/-}$ (male and female) mice were i.p. infected with 2×10^6 PFU of ZIKV (or DENV-2) or 10^5 PFU of ZIKV (or DENV-2), respectively. In all experiments, mice receiving PBS buffer were used as the mock-treated controls. Survival, weight loss, and disease signs were monitored.

Peptide prediction approaches and peptide synthesis. MHC class I peptide binding affinity predictions were performed using the Immune Epitope Database (IEDB) Tools website with the "IEDB-recommended" method selection. Predicted binding affinities for all nonredundant 8- to 9-mer peptides that bound H2-Kb and H2-Db were obtained. For each allele, the lists of peptides obtained above were sorted by increasing consensus percentile rank and restricted to 0.8. All of the synthesized peptides were obtained from Scilight Biotechnology Co., Ltd. (Beijing, China). The purity of the synthesized peptides was >98%, as determined by high-performance liquid chromatography analysis.

Flow cytometry analyses. All antibodies were purchased from eBioscience. Red blood cells (RBCs) were lysed using RBC lysis buffer (eBioscience). For surface staining, splenocytes or lymphocytes were washed and then incubated with anti-CD8-PerCP/AF780, anti-CD44-PE, anti-CD62L-PerCP, anti-CD11a-FITC/Efluor450, or anti-CD49d-PerCP at 4°C in the dark. For intracellular cytokine staining, 1.5×10^6 splenocytes were plated in 96-well U-bottom plates and stimulated with individual ZIKV peptides (5 μg/ml) in the presence of brefeldin A (eBioscience) for 5 h. For CD107a staining, CD107a-FITC was added to the wells at the same time as the peptide. The cells were washed, and surface staining was performed. The cells were then fixed and permeabilized using a BD Biosciences Cytofix/Cytoperm kit and stained with anti-IFN-γ/APC or anti-IFN-γ/PE. Samples were read on a FACSCanto II or LSR Fortessa (BD Biosciences) and analyzed using FlowJo software.

Virus-specific IFN-γ-producing CD8$^+$ T cell detection. Splenocytes (1.5×10^6) harvested from ZIKV-infected mice were stimulated with DC2.4 that had been treated with heat-inactivated ZIKV 12 h previously. After 18 h brefeldin A was added, and after 5 h the cells were analyzed by flow cytometry.

***In vivo* cytotoxicity assay.** Five-week-old B6 mice (recipients) were infected with 2×10^6 PFU of ZIKV. Splenocytes (targets) were harvested from naive donor B6 mice 7 days later. The RBCs were lysed, and the target cells were pulsed with 1 μg of the irrelevant peptide ($OVA_{257–264}$) and the positive peptide of ZIKV per ml for 1 h at 37°C. The cells were then washed. ZIKV peptide-pulsed cells were labeled with 1 μM CFSE (CFSE^{high}), and the irrelevant peptide-pulsed cells were labeled with 100 nM CFSE (CFSE^{low}) at 37°C for 10 min. After washing, the two cell populations were mixed in a 1:1 ratio, and 5×10^6 cells from each population were injected i.v. into naive or infected recipient mice. After 13 h, the mice were sacrificed, and splenocytes were analyzed by flow cytometry, with gating on the CFSE$^+$ cells. The killing percentage was calculated as follows: 100 − [(% ZIKV peptide-stimulated in infected mice/% irrelevant peptide-stimulated in infected mice)/(% ZIKV peptide-stimulated in naive mice/% irrelevant peptide-stimulated in naive mice) × 100].

Lymphocyte cell isolation from CNS. ZIKV-infected mice were sacrificed at the indicated time points and immediately perfused with PBS. CNS-infiltrating lymphocytes were isolated using mechanical disruption of the organ, followed by enrichment on 70 to 30% Percoll gradients (GE Healthcare) and centrifugation for 20 min at 800 × *g*. The median-layer lymphocytes were obtained.

Adoptive transfer of CD8$^+$ T cells. ZIKV-infected CD8$^+$ T cells were isolated from B6 mice on day 7 after infection with 2×10^6 PFU of ZIKV using a magnetic CD8$^+$ T cell selection kit (CD8a Ly-2; Miltenyi Biotech). Noninfected CD8 T cells were isolated from noninfected B6 mice as described above. A total of 10^7 CD8$^+$ T cells were transferred into 5-week-old naive *Ifnar1*$^{-/-}$ mice, and recipient mice were infected with 10^5 PFU of ZIKV 1 day after cell transfer. Further studies were performed after infection.

Quantitation of the ZIKV and DENV burden in mice. For viral RNA detection, tissues were homogenized, and total RNA was extracted using TRIzol reagent (Invitrogen). cDNA was prepared from 1 μg of RNA using 10 U of avian myeloblastosis virus reverse transcriptase (Promega, USA), a deoxynucleoside triphosphate mixture, and oligo(dT) primers at 37°C for 1 h. Real-time qRT-PCR was performed on an ABI 7500 (Applied Biosystems, USA) using SYBR green Supermix (Applied Biosystems) according to the manufacturer's protocol. The expression levels of viral RNA were normalized against HPRT (hypoxanthine phosphoribosyltransferase). Quantitative RT-PCR experiments were performed using three independent RNA preparations. The real-time PCR primers set for ZIKV RNA detection were as follows: forward (5′-TGAYAAGCARTCAGACAC-3′) and reverse (5′-TCACCARRCTCCCTTTGC-3′). For DENV-2, the primer set was as follows: forward (5′-CAGGCTATGGCACTGTCACGAT-3′) and reverse (5′-CCATTTGCAGC AACACCATCTC-3′).

Plaque-forming assay. Infectious viruses in mouse tissues were determined by a standard plaque-forming assay in BHK-21 monolayers in six-well plates. In brief, the tissues were homogenized and centrifuged at 4°C, and then serial 10-fold dilutions of the supernatant were inoculated onto BHK cells. After 1 h of adsorption at 37°C, the wells were overlaid with 1 ml of DMEM supplemented with 2% FBS and 1% agarose. The plates were incubated for 4 days at 37°C in 5% CO_2. Monolayers were fixed by the addition of 1 ml of 4% formalin solution to the overlay medium. After 1 h of fixation at room temperature, the fixative was removed, the wells were washed with water, and the monolayers were stained with 1% crystal violet in 70% methanol. The plaques were counted, and titers are expressed as PFU per ml or per g.

Tetramer preparation and cell staining. H-2Db-restricted tetramers of peptides $E_{4–12}$ were prepared as previously described (36). Briefly, to produce biotinylated peptide-MHC protein, H-2Db was modified by the addition of a substrate sequence for the biotinylating enzyme BirA at the C terminus of the a3 domain. *In vitro*-renatured H-2Db/peptide complexes were then purified and biotinylated by incubation with D-biotin, ATP, and the biotin protein ligase BirA (Avidity) at 4°C for 12 h. The biotinylated H-2Kd was further purified over a Superdex 200 10/300 GL gel filtration column (GE Healthcare) to remove excess biotin and then mixed with PE-streptavidin (Sigma-Aldrich). Cells from the subjects were stained with PE-tetramer and FITC-conjugated anti-CD11a, APC-conjugated anti-CD3, and APC-CY7-conjugated anti-CD8 AbS. All samples were analyzed with a FACSCalibur or Fortessa flow cytometer (BD Biosciences) after staining.

Statistical analysis. All data were analyzed using GraphPad Prism software. A Student *t* test was used to analyze differences in mean values between groups. All results are expressed as means ± the standard errors of the mean (SEM). *P* values of <0.05 were considered statistically significant (*, $P < 0.05$; **$P < 0.01$, ***, $P < 0.001$; ****, $P < 0.0001$).

ACKNOWLEDGMENTS

This study was supported by National Key Research and Development Project grant 2016YFC1200302, National Key Research and Development Program of China grant 2017YFC1200202, the Zika Special Project of the Ministry of Science and Technology Reform and Development Project, and the External Cooperation Program of Chinese Academy of Sciences (grant 153211KYSB20160001). G.F.G. is a leading principal investigator of the NSFC Innovative Research group (grant 81621091).

We thank Mingzhao Zhou for his donation of the DC2.4 cell line and Cheng-Feng Qin for providing the DENV-2 virus.

REFERENCES

1. Sharma A, Lal SK. 2017. Zika virus: transmission, detection, control, and prevention. Front Microbiol 8:110. https://doi.org/10.3389/fmicb.2017.01602.
2. Dick GW, Kitchen SF, Haddow AJ. 1952. Zika virus I Isolations and serological specificity. Trans R Soc Trop Med Hyg 46:509–20. https://doi.org/10.1016/0035-9203(52)90042-4.
3. Mlakar J, Korva M, Tul N, Popovic M, Poljsak-Prijatelj M, Mraz J, Kolenc M, Resman Rus K, Vesnaver Vipotnik T, Fabjan Vodusek V, Vizjak A, Pizem J, Petrovec M, Avsic Zupanc T. 2016. Zika virus associated with microcephaly. N Engl J Med 374:951–958. https://doi.org/10.1056/NEJMoa1600651.
4. Lucchese G, Kanduc D. 2016. Zika virus and autoimmunity: from microcephaly to Guillain-Barre syndrome, and beyond. Autoimmun Rev 15:801–808. https://doi.org/10.1016/j.autrev.2016.03.020.
5. Elong Ngono A, Vizcarra EA, Tang WW, Sheets N, Joo Y, Kim K, Gorman MJ, Diamond MS, Shresta S. 2017. Mapping and role of the CD8+ T cell response during primary Zika virus infection in mice. Cell Host Microbe 21:35–46. https://doi.org/10.1016/j.chom.2016.12.010.
6. Lazear HM, Govero J, Smith AM, Platt DJ, Fernandez E, Miner JJ, Diamond MS. 2016. A mouse model of Zika virus pathogenesis. Cell Host Microbe 19:720–730. https://doi.org/10.1016/j.chom.2016.03.010.
7. Manangeeswaran M, Ireland DD, Verthelyi D. 2016. Zika (PRVABC59) infection is associated with T cell infiltration and neurodegeneration in CNS of immunocompetent neonatal C57Bl/6 mice. PLoS Pathog 12:e1006004. https://doi.org/10.1371/journal.ppat.1006004.
8. Winkler CW, Myers LM, Woods TA, Messer RJ, Carmody AB, McNally KL, Scott DP, Hasenkrug KJ, Best SM, Peterson KE. 2017. Adaptive immune responses to Zika virus are important for controlling virus infection and preventing infection in brain and testes. J Immunol 198:3526–3535. https://doi.org/10.4049/jimmunol.1601949.
9. Pardy RD, Rajah MM, Condotta SA, Taylor NG, Sagan SM, Richer MJ. 2017. Analysis of the T cell response to Zika virus and identification of a novel CD8+ T cell epitope in immunocompetent mice. PLoS Pathog 13:e1006184. https://doi.org/10.1371/journal.ppat.1006184.
10. Zust R, Toh YX, Valdes I, Cerny D, Heinrich J, Hermida L, Marcos E, Guillen G, Kalinke U, Shi PY, Fink K. 2014. Type I interferon signals in macrophages and dendritic cells control dengue virus infection: implications for a new mouse model to test dengue vaccines. J Virol 88:7276–7285. https://doi.org/10.1128/JVI.03827-13.
11. Wen J, Tang WW, Sheets N, Ellison J, Sette A, Kim K, Shresta S. 2017. Identification of Zika virus epitopes reveals immunodominant and protective roles for dengue virus cross-reactive CD8+ T cells. Nat Microbiol 2:17036. https://doi.org/10.1038/nmicrobiol.2017.36.
12. Hastings AK, Erickson JJ, Schuster JE, Boyd KL, Tollefson SJ, Johnson M, Gilchuk P, Joyce S, Williams JV. 2015. Role of type I interferon signaling in human metapneumovirus pathogenesis and control of viral replication. J Virol 89:4405–4420. https://doi.org/10.1128/JVI.03275-14.
13. Pinto AK, Daffis S, Brien JD, Gainey MD, Yokoyama WM, Sheehan KC, Murphy KM, Schreiber RD, Diamond MS. 2011. A temporal role of type I interferon signaling in CD8+ T cell maturation during acute West Nile virus infection. PLoS Pathog 7:e1002407. https://doi.org/10.1371/journal.ppat.1002407.
14. Contreras D, Arumugaswami V. 2016. Zika virus infectious cell culture system and the in vitro prophylactic effect of interferons. J Vis Exp https://doi.org/10.3791/54767.
15. Bowen JR, Quicke KM, Maddur MS, O'Neal JT, McDonald CE, Fedorova NB, Puri V, Shabman RS, Pulendran B, Suthar MS. 2017. Zika virus antagonizes type I interferon responses during infection of human dendritic cells. PLoS Pathog 13:e1006164. https://doi.org/10.1371/journal.ppat.1006164.
16. McDermott DS, Varga SM. 2011. Quantifying antigen-specific CD4 T cells during a viral infection: CD4 T cell responses are larger than we think. J Immunol 187:5568–5576. https://doi.org/10.4049/jimmunol.1102104.
17. Rai D, Pham NL, Harty JT, Badovinac VP. 2009. Tracking the total CD8 T cell response to infection reveals substantial discordance in magnitude and kinetics between inbred and outbred hosts. J Immunol 183:7672–7681. https://doi.org/10.4049/jimmunol.0902874.
18. Groom JR, Luster AD. 2011. CXCR3 in T cell function. Exp Cell Res 317:620–631. https://doi.org/10.1016/j.yexcr.2010.12.017.
19. Wang Q, Yang Y, Zheng H, Bi Y, Song J, Li L, Gu D, Wang P, Li S, Liu S, Zhao Y, Liu L, Gao G, Liu Y. 2016. Genetic and biological characterization of Zika virus from human cases imported through Shenzhen Port. Chin Sci Bull 61:2463–2474. https://doi.org/10.1360/N972015-00990.
20. Diamond MS. 2003. Evasion of innate and adaptive immunity by flaviviruses. Immunol Cell Biol 81:196–206. https://doi.org/10.1046/j.1440-1711.2003.01157.x.
21. Yauch LE, Prestwood TR, May MM, Morar MM, Zellweger RM, Peters B, Sette A, Shresta S. 2010. CD4+ T cells are not required for the induction of dengue virus-specific CD8+ T cell or antibody responses but contribute to protection after vaccination. J Immunol 185:5405–5416. https://doi.org/10.4049/jimmunol.1001709.
22. Harrison SC. 2016. Immunogenic cross-talk between dengue and Zika viruses. Nat Immunol 17:1010–1012. https://doi.org/10.1038/ni.3539.
23. Stettler K, Beltramello M, Espinosa DA, Graham V, Cassotta A, Bianchi S, Vanzetta F, Minola A, Jaconi S, Mele F, Foglierini M, Pedotti M, Simonelli L, Dowall S, Atkinson B, Percivalle E, Simmons CP, Varani L, Blum J, Baldanti F, Cameroni E, Hewson R, Harris E, Lanzavecchia A, Sallusto F, Corti D. 2016. Specificity, cross-reactivity, and function of antibodies elicited by Zika virus infection. Science 353:823–826. https://doi.org/10.1126/science.aaf8505.
24. Yauch LE, Zellweger RM, Kotturi MF, Qutubuddin A, Sidney J, Peters B, Prestwood TR, Sette A, Shresta S. 2009. A protective role for dengue virus-specific CD8+ T cells. J Immunol 182:4865–4873. https://doi.org/10.4049/jimmunol.0801974.
25. Kaech SM, Wherry EJ, Ahmed R. 2002. Effector and memory T-cell differentiation: implications for vaccine development. Nat Rev Immunol 2:251–262. https://doi.org/10.1038/nri778.
26. Krzych U, Dalai S, Zarling S, Pichugin A. 2012. Memory CD8 T cells specific for plasmodia liver-stage antigens maintain protracted protection against malaria. Front Immunol 3:370. https://doi.org/10.3389/fimmu.2012.00370.
27. Moseman EA, McGavern DB. 2013. The great balancing act: regulation and fate of antiviral T-cell interactions. Immunol Rev 255:110–124. https://doi.org/10.1111/imr.12093.
28. Ransohoff RM, Engelhardt B. 2012. The anatomical and cellular basis of immune surveillance in the central nervous system. Nat Rev Immunol 12:623–635. https://doi.org/10.1038/nri3265.
29. Malkki H. 2016. CNS infections: Zika virus infection could trigger Guillain-Barre syndrome. Nat Rev Neurol 12:187. https://doi.org/10.1038/nrneurol.2016.30.
30. Hou HQ, Miao J, Feng XD, Han M, Song XJ, Guo L. 2014. Changes in lymphocyte subsets in patients with Guillain-Barre syndrome treated with immunoglobulin. BMC Neurol 14:202. https://doi.org/10.1186/s12883-014-0202-3.
31. Aliota MT, Caine EA, Walker EC, Larkin KE, Camacho E, Osorio JE. 2016. Characterization of lethal Zika virus infection in AG129 mice. PLoS Negl Trop Dis 10:e0004682. https://doi.org/10.1371/journal.pntd.0004682.
32. Rossi SL, Tesh RB, Azar SR, Muruato AE, Hanley KA, Auguste AJ, Langsjoen RM, Paessler S, Vasilakis N, Weaver SC. 2016. Characterization of a novel murine model to study Zika virus. Am J Trop Med Hyg 94:1362–1369. https://doi.org/10.4269/ajtmh.16-0111.
33. Korn T, Kallies A. 2017. T cell responses in the central nervous system. Nat Rev Immunol 17:179–194. https://doi.org/10.1038/nri.2016.144.
34. Cupovic J, Onder L, Gil-Cruz C, Weiler E, Caviezel-Firner S, Perez-Shibayama C, Rulicke T, Bechmann I, Ludewig B. 2016. Central nervous system stromal cells control local CD8+ T cell responses during virus-induced neuroinflammation. Immunity 44:622–633. https://doi.org/10.1016/j.immuni.2015.12.022.
35. Wang Q, Yang H, Liu X, Dai L, Ma T, Qi J, Wong G, Peng R, Liu S, Li J, Li S, Song J, Liu J, He J, Yuan H, Xiong Y, Liao Y, Yang J, Tong Z, Griffin BD, Bi Y, Liang M, Xu X, Qin C, Cheng G, Zhang X, Wang P, Qiu X, Kobinger G, Shi Y, Yan J, Gao GF. 2016. Molecular determinants of human neutralizing antibodies isolated from a patient infected with Zika virus. Sci Transl Med 8:369ra179. https://doi.org/10.1126/scitranslmed.aai8336.
36. Liu J, Wu B, Zhang S, Tan S, Sun Y, Chen Z, Qin Y, Sun M, Shi G, Wu Y, Liu N, Ning K, Ma Y, Gao B, Yan J, Zhu F, Wang H, Gao GF. 2013. Conserved epitopes dominate cross-CD8+ T-cell responses against influenza A H1N1 virus among Asian populations. Eur J Immunol 43:2055–2069. https://doi.org/10.1002/eji.201343417.